Tweedle proteins form extracellular 2D-structures defining body and cell shape in *Drosophila melanogaster*

Renata Zuber[1,2], Yiwen Wang[2], Nicole Gehring[2], Slawomir Bartoszewski[3] and Bernard Moussian[1,4,*]

1 Applied Zoology, Technical University of Dresden, Zellescher Weg 20b, 01062 Dresden, Germany

2 Interfaculty Institute for Cell Biology (Ifiz), University of Tübingen, Auf der Morgenstelle 15, 72076 Tübingen, Germany

3 Rzeszow University, Department of Biochemistry and Cell Biology, ul. Zelwerowicza 4, 35-601 Rzeszów, Poland

4 Institut Biologie Valrose (iBV), Université Nice Sophia Antipolis, Parc Valrose, Nice Cedex, France

Abstract

Tissue function and shape rely on the organisation of the extracellular matrix (ECM) produced by the respective cells. Here, we report on our study on the function of the extracellular Tweedle proteins (Twdl) in the fruit fly *Drosophila melanogaster* during shaping of the integument composed of the epidermis and its apical extracellular cuticle. We show that Twdl proteins form at least two adjacent two-dimensional sheets underneath the cuticle surface by self-assembly. Dominant mutations in two *twdl* genes *Tubby*^{1} and *TwdlL*^{93} cause ectopic spherical accumulation of Twdl proteins within lower cuticle regions. These aggregates recruit also non-mutated Twdl proteins. Thus, the mutated residues are needed for the plane arrangement of Twdl proteins and their localisation underneath the cuticle surface without affecting their ability to self-assembly. Depletion of Twdl proteins from the sub-surface region and their ectopic accumulation are associated with the disruption of the ridged profile of the plasma membrane-cuticle interface region and lateral instead of longitudinal stretching of epidermal cells. Based on these data, we propose that depletion of Twdl proteins from the sub-surface region entails weakening of the cuticle resistance against the internal hydrostatic pressure that according to Barlow's law in turn causes lateral expansion of the body. Interestingly, these changes do not provoke crawling defects suggesting that body shape and locomotion require separate cuticle properties.

Introduction

Extracellular matrices (ECM) contribute to the geometry and consistency of cells and tissues. Generally, the role of an ECM depends on its components and their interactions that ultimately define its organisation. Cartilaginous tissues, for instance, consist of a random distribution of the extracellular polysaccharide hyaluronic acid and associated proteins including collagen and aggrecan produced and secreted by embedded chondrocytes [1-4]. Tension applied on this kind of tissues in concert with swelling forces entail the arrangement of the components and, finally, the shape of the tissue.

A less well studied ECM is the cuticle of insects that outlines the shape of the organism. In some body regions such as the head capsule of caterpillars or the protective elytra of adult beetles, the hardness of the exoskeleton is sufficient to sustain the required shape. In some other body regions such as the ventral abdomen of many adult insects or the larval body, the respective shape does not only depend on the exoskeleton, but involves the inner hydrostatic pressure. Despite these differences the principal organisation of the cuticle is well conserved in different body

regions and among species. The prototype of the cuticle consists of three composite horizontal layers, the outermost envelope, the middle epicuticle and the inner procuticle [5, 6].

Like cartilaginous tissues, the procuticle is composed of an extracellular polysaccharide, namely chitin, and associated proteins. In the last few years, data accumulated underlining that the proteins binding to chitin and their partners together specify the physical properties of the cuticle. In the elytral procuticle of the red flour beetle *Tribolium castaneum*, for instance, the chitin-binding proteins Cpr27 and Cpr18 associate with chitin and interact with the cuticle protein CP30 probably over covalent N-□-alanyl-dopamine (NBAD) bridges that are catalysed by the phenoloxidase TmLaccase2 [7, 8]. This arrangement correlates with the stiffness of the elytral cuticle. In the fruit fly *Drosophila melanogaster*, proteins such as the chitin-binding and elastic protein Resilin in the contact region between the procuticle and the epicuticle are cross-linked to each other via dityrosine bonds [9]. The formation of this sub-layer involves the C-type lectin Schlaff (Slf) and a yet unknown peroxidase. The exact underlying molecular mechanisms are not understood. Besides its function as a barrier, the dityrosine sub-layer may also be important for cuticle elasticity.

In order to deepen our understanding of the mechanisms of cuticle ECM organisation, we have studied the function of several members of a class of cuticle proteins named Tweedle (Twdl) in the fruit fly *Drosophila melanogaster* [10]. Twdl proteins are characterised by an N-terminal signal peptide and a domain with four conserved blocks (DUF243), but do not display any homology to any other entry in protein databases. Deletions of stretches of amino acids of these domains provoke body shape changes in larvae and adult flies. In brief, we show that Twdl proteins localise to the epicuticle and assist the organisation of the epicuticle-procuticle interface, which we hypothesise to be responsible for defining the body shape.

Here, we show that Twdl proteins localise to the epicuticle forming at least two 2-dimensional sheets. In addition, we demonstrate that Twdl proteins with deletions in the DUF243 domain form ectopic aggregates within the procuticle. These aggregates recruit non-mutated Twdl proteins as well as proteins from the procuticle-epcuticle interface. We propose that this mis-organisation entails changes in the physical properties of the cuticle that as a consequence dilates laterally rather than longitudinally, thereby facilitating lateral growth and conferring squat larval shape.

Materials & Methods

Fly husbandry

Flies were kept in cages with apple juice agar plates with yeast, from which embryos and larvae were collected. Embryonic stages were recognized according to the gut morphology described by Hartenstein and Campos-Ortega [11]. Homozygous mutants non-carrying any GFP- or YFP- constructs were identified from the rest of the embryos that were heterozygous or homozygous for the balancer chromosome expressing GFP (Dfd:YFP or Kr:GFP). Collected embryos were dechorionated in chlorine bleach diluted 1:1 in tap water, manually freed from the vitelline membrane or left in the vitelline membrane, subsequently mounted in Voltalef 10S oil (VWR Chemicals) and observed by microscopy.

Transgenic flies harbouring constructs were generated by the BestGene Inc (USA) company. The constructs used are: *knkp*:*cpr67Fa-rfp* with the promoter of the *knk* gene [12] upstream of the coding region of *cpr67Fa* fused to the open reading frame of *rfp* in pW8; TwdlD-RFP-NLS with the coding regions of *twdlD* and *rfp-nls* fused

together and downstream of the *twdlD* promoter [9] in pW8, Tb-GFP and TwdlS-GFP from the Flyfos library [13], Tb1-RFP [14], TwdlF-dsRed and TwdlD-dsRed [10], UAS:Verm-RFP [15] and Obst-E-GFP [16]. The Gal4 line to drive UAS:*verm-rfp* expression was *daughterless*:Gal4.

Molecular biology

In order to identify a mutation in TwdlL gene standard PCR reaction and sequencing were performed.

Genetics

In order to down-regulate the activity of respective Tweedle proteins, RNAi technique and UAS:Gal4 system were used. Flies carrying respective UAS:RNAi constructs were crossed to the ones bearing ubiquitously expressed Gal4 (*daughterless:*Gal4). The larval and pupal phenotype of the progeny was observed.

For confirmation that Tb^{1} and Tb^{93} mutations are not alleles of the same gene we performed the complementation test by crossing them with each other, subsequently crossing the F1 females with the wild-type males and counting the number of the wild-type, non-Tb looking pupae.

Microscopy and image preparation

For live imaging, larvae were anesthesised with ether, mounted in halocarbon 700 or 50% glycerol and observed either by confocal laser scanning microscopy (CLSM, using Zeiss LSM 710, 780 and 880) or fluorescent binocular Leica M205 FA.

For imaging of the cuticle preparations, the larvae were mounted in Hoyer's medium (30 g gum arabic, 50 ml distilled water, 200 g chloral hydrate, 20 g glycerol, mixed 1:1 with lactic acid), kept overnight at 65°C and observed on a binocular Leica M205 FA. Transmission electron microscopy was performed following our extensive protocol published in 2010 [17]. For examination of the cuticular ridges, third instar larvae were digested in Hoyer's medium and their cuticles washed several times in the distilled water. Afterwards they were stacked to the metal plate and their inner side was scanned by the atomic force microscope (Innova AFM, Bruker).

For figures preparation Adobe Photoshop CS3 and Adobe Illustrator CS4 softwares were used without changing initial microscope settings. For cell measurements AxioVision Rel. 4.7 was used.

Body length measurements

Third instar larvae were placed on the agar plate and the movie of 10 steps (1 step = contraction and subsequent stretching) was made. Afterwards in every step the body in the most contracted and stretched state was measured and the difference between shortest and the longest measurement of all 10 steps of 5 wild-type, homozygous Tb^{1} and Tb^{93} larvae were counted and compared.

Movement measurements

100 third instar wild-type, homozygous $Tb^{1}$and Tb^{93} larvae were placed into the vials with agar food, 20 larvae of each kind to one vial. After pupariation of all larvae the distance between the pupae on the vial wall and the food level was measured and the average of measurements of 20 larvae was determined.

Results

Twdl proteins are expressed at different time points during development

To study the cellular function of Twdl proteins, we first determined the expression pattern of transgenic flies expressing fluorescent-tagged versions of the candidates TwdlA-GFP (Tb-GFP), TwdlD-dsRed, TwdlF-dsRed and TwdlS-GFP under the control of their endogenous promoters (Fig.1).
Tb-GFP starts to be expressed in the late embryo in patches in the lateral epidermis. Later, during larval development, its expression is detected in the entire epidermis. The TwdlS-GFP signal is barely visible in the cuticle of L2 larvae and becomes more intense in the whole cuticle of L3 larvae. TwdlF-dsRed is localized in the whole cuticle at all three larval stages. TwdlD-dsRed is expressed in the epidermis during the first two larval stages, but is excluded from the segmental grooves. At the third larval stage, only a very faint TwdlD-dsRed signal at the posterior part is detected.
In summary, Twdl proteins are expressed at different time points during development in different, partially overlapping regions of the epidermis.

Twdl proteins mark the epicuticle

In order to determine the sub-cuticular localization of Twdl proteins, we analysed the distribution of the three fluorescent-tagged Twdl proteins, i.e. Tb-GFP, TwdlF-dsRed and TwdlS-GFP in the cuticle of live L3 larvae by confocal microscopy (Fig. 2, 3, 4). We used the auto-fluorescence of the cuticle surface excited with a 405 nm laser and the tagged procuticle markers Cuticle Protein R&R 67b (CPR67b-dsRed) and Vermiform (Verm-RFP) as landmarks. GFP-conjugated TwdlS was located between the 405 signal and the broad CPR67b-dsRed or Verm-RFP region marking the procuticle (Fig. 2). TwdlF-dsRed was detected in layer above the TwdlS-GFP but below the 405-signal (Fig. 3). Tb-GFP overlapped with TwdlF-dsRed (Fig. 4). We conclude that these Twdl proteins belong to the epicuticle subdividing it into distinct horizontal domains.
To test this conclusion, we monitored the expression of TwdlF-dsRed in embryos deficient for ecdysone that we had previously shown to be necessary for epicuticle differentiation [12]. In wild-type embryos, TwdlF-dsRed is detected in the entire larval cuticle (Fig. 6). In embryos mutant for *phantom* (*phm*) that codes for a P450 enzyme acting in the ecdysone biosynthesis pathway, TwdlF-dsRed is hardly expressed. Sporadically, dots of an RFP signal are found within epidermal cells. This finding is consistent with our conclusion that Twdl proteins localise to the epicuticle. Moreover, this result also indicates that activation of the *twdlF* promoter depends on ecdysone signalling.

Twdl proteins bind selectively to aggregates formed in Tb mutant larvae

To unravel the role of Twdl proteins in epicuticle formation and structure, we analysed the distribution of the fluorescent-tagged Twdl proteins in *Tb* mutant i.e. Tb^{1} and Tb^{93} larvae. In Tb^{1} larvae, TwdlS-GFP, Tb-GFP and TwdlF-dsRed are partially localized correctly in the epicuticle and partially aggregated in the procuticle (Fig. 2, 3, 4). In the cuticle of Tb^{93} larvae, the signal of aggregated TwdlS-GFP and Tb-GFP is weaker compared to the signal in the Tb1 mutant larvae, whilst TwdlF-dsRed binds the aggregates very weakly or does not bind them at all (Fig. 2, 3, 4).
In order to find out whether the origin of the aggregates may be a mutated Tb protein, we compared the distributions of non-mutated, GFP-tagged and mutated, RFP-tagged versions of Tb, Tb-GFP and Tb^{1}-RFP [14], respectively, in the cuticle of live L3 larvae (Fig. 4). Tb^{1}-RFP formed aggregates in the cuticle of these larvae. Co-

expressed Tb-GFP was recruited to these aggregates. To test whether other Twdl proteins might be part of the Tb^1-RFP aggregates, we co-expressed Tb^1-RFP with TwdlS-GFP (Fig. 4). The TwdlS-GFP signal overlaps with the signal of the Tb^1-RFP aggregates. We conclude that mutated Tb forms aggregates within the cuticle, which are able to recruit non-mutated Twdl proteins including Tb itself, TwdlD, TwdlF and TwdlS.

The Tb^{93} is a twdlL allele

The differences in the localisation of TwdlF-dsRed, TwdlS-GFP and Tb-GFP in both *Tb^1* and *Tb^{93}* alleles suggest that this discrepancy may be a consequence of different mutations in the *Tb* gene. Indeed, the phenotypes caused by these two alleles differ also between the larval stages. *Tb^1* larvae start to show the squat phenotype at the L2 larval stage, whilst *Tb^{93}* already at L1 (supplementary data 1).
The *Tb^1* allele carries a deletion removing six amino acids within the DUF 243 domain [9]. Sequencing of the *Tb* gene in the *Tb^{93}* genome revealed no changes in the Tb protein sequence (data not shown). We reckoned, therefore, that *Tb^{93}* is not an allele of *Tb*. To test this notion, we sought to recombine the *Tb^1* and *Tb^{93}* alleles on one chromosome arguing that recombination would underline that these mutations affect different loci. For this purpose, in a population issued from a cross of *Tb^1* and *Tb^{93}* heterozygous flies segregating both mutations in trans, we screened for larvae that did not show the squat phenotype. We isolated four non-Tb larvae in a population of 5860 larvae suggesting that the mutations affect different loci and that these loci are roughly 0,1 cM apart. Based on this result, we sequenced other *twdl* genes in the *twdl* cluster on the right arm of chromosome 3 in *Tb^{93}* animals in order to identify the mutation responsible for the phenotype. Indeed, we found a missense mutation in the sequence coding for a conserved amino acid of the DUF 243 domain in another *Twdl* gene, *TwdlL* (Supplementary fig.2). In order to confirm that the *Tb^{93}* phenotype is caused by the mutation in the *TwdlL* gene, we expressed a hairpin RNA directed against the *twdlL* gene in the background of *Tb^{93}*. The hairpin RNA abolished the squat phenotypes of *Tb^{93}* larvae and pupae. In contrast, hairpin RNA against *TwdlL* did not cause any changes in the phenotype of *Tb^1* animals. As a control, we also tested several hairpin RNAs against other *twdl* genes in the *Tb^{93}* background. No phenotype changes were observed in any of these crosses. We conclude that *Tb^{93}* is a dominant allele of the *twdlL* gene. Taken together, Tb and TwdlL are both needed for correct epicuticle formation.

Twdl aggregates constitute an ectopic epicuticle immersed in the procuticle

The aggregates visible on optical cross-sections of the cuticle shown in figures 3 and 4 do not localise to the expected region of the epicuticle just below the surface but scattered along the z-axis of the cuticle (Fig. 3, 4). To precisely localise these aggregates, we analysed the ultrastructure of the *Tb^1* and *Tb^{93}* larval cuticle by transmission electron microscopy. (data not shown). We observed electron-dense aggregates immersed within the procuticle.
To verify whether these inclusions might be the same structures as the aggregates identified by confocal microscopy, TwdlS-GFP was co-expressed with fluorescent-tagged chitin-binding proteins CPR67b-RFP and Vermiform-RFP (Fig.2) in *Tb^1* mutant larvae. In both cases the TwdlS-GFP aggregates were surrounded by the respective red fluorescing procuticle marker.
Taken together, we conclude that Twdl proteins form an ectopic epicuticle within the procuticle of *Tb^1* and *Tb^{93}* larvae.

Twdl function in hairs differs from their function in naked cuticle

Organisation of the cuticle in dorsal hairs of wild type larvae is similar to the naked cuticle: Twdl proteins form layers under the blue auto-fluorescent layer (Fig. 5). The procuticle is located in the middle of a hair and reaches its tip. In the *twdl* mutant background Twdls accumulate at the tips of the hair. The procuticle still remains in the middle of the hair, except for the tip, so that these two layers (Twdl and procuticle) do not overlap.

Resilin associates with the margin of Twdl aggregates

Recently, we showed that the contact zone between the epicuticle and the procuticle is marked by dityrosinylated proteins in *D. melanogaster* larvae [18]. In the *wild-type* third instar one-day-old larvae, Resilin-Venus representing the dityrosinylated layer localizes beneath the TwdlF-dsRed layer (Fig. 7). In the Tb^{1} and Tb^{93} mutant larvae at the same stage, Resilin-Venus is attracted to the aggregates and encases them. In the dorsal hairs of the young *wild type* third instar larvae just after hatching Resilin-Venus occupies the space below the TwdlF-dsRed layer in the dorsal hair, while in the hairs of the Tb^{1} and Tb^{93} mutant larvae, it accumulates also at the hair tips, where the aggregated Tweedle proteins occur. In one-day-old third instar *wild-type* larvae localization of Resilin-Venus is unchanged compared to young third instar larvae, whilst in one-day-old Tb^{1} and Tb^{93} mutant larvae Resilin-Venus is not localised at the hair tips anymore but encases the Twdl-aggregates the hair tip. Thus, Twdl proteins dictate the localization and the shape of the dityrosinylated layer between the epicuticle and the procuticle.

Non-cell autonomous localization of the aggregated Twdls in the cuticle

In our live localization experiments, we noticed that, as reported, TwdlD-RFP was expressed in a striped pattern in wild-type larvae. Dorsal hairs were lacking TwdlD-RFP. In the cuticle of Tb^{1} and $TwdlL^{93}$ larvae (Fig.8), the Twdl aggregates were visible in the areas of dorsal hairs including the tips of hairs. Two alternative scenarios may explain this observation. Either the expression pattern of *twdlD* was changed in Tb^{1} and $TwdlL^{93}$ larvae, or, in addition to the vertical, the lateral mobility of the TwdlD within the cuticle was enhanced in these larvae. In order to distinguish between these two possibilities, we monitored the expression of a nuclear-binding RFP under the control of the *TwdlD* promoter (TwdlD>RFP-NLS) in wild-type, Tb^{1} and $TwdlL^{93}$ larvae. In all three cases RFP-NLS was detected in a striped pattern in the epidermis of developing embryos and larvae. This finding indicates that there were no changes in the expression pattern of *twdlD*. Thus, the occurrence of the aggregates in the whole cuticle was due to the lateral spreading of the protein in the extracellular space.

Epidermal cell shape is altered in Twdl mutant larvae

Compared to wild-type larvae, Tb^{1} and $TwdlL^{93}$ mutant larvae are wider, but shorter. To study to what extent the body shape difference is reflected at the cellular level in Tb^{1} and $TwdlL^{93}$ larvae, we examined the shapes of their epidermal cells visualised by the membrane bound CD8-GFP protein. In all larvae tested, the number of cells and their average area were unchanged, but the shape of the cells was significantly altered in Tb^{1} and $TwdlL^{93}$ larvae (Fig.9, Supplementary fig.3). These cells were

shorter along the anterior-posterior axis and longer along the dorso-ventral axis of the animal as compared with cells of wild-type larvae.

Cuticle stretchability and movement capabilities of the Tb^1 and $TwdlL^{93}$ larvae are unchanged

An intact exoskeleton is a prerequisite for insect locomotion. To find out whether the altered body shape of Tb^1 and $TwdlL^{93}$ larvae affects crawling efficiency, we measured the ratio of the body length in the most stretched to the most contracted state of young third instar wild-type and Tb^1 and $TwdlL^{93}$ larvae (Suppl. Fig. 5). We observed there was no significant difference between the ratios of the wild-type and Tb^1 and $TwdlL^{93}$ larvae.

We also investigated whether the barrel-like larval shape limits the crawling capabilities of the Tb^1 and $TwdlL^{93}$ larvae. For this purpose, we measured the height on which larvae formed pupae on the vial wall. We found that in all cases, the wild-type, Tb^1 and $TwdlL^{93}$ homozygous larvae, the average pupariation height was comparable (Suppl. Fig.5).

Taken together, we conclude that the stretchiness of the cuticle of the Tb^1 and $TwdlL^{93}$ larvae and their movement efficiency are unchanged.

Basal cuticular ridges are disorganised in Tb^1 and $TwdlL^{93}$ mutant larvae

The cuticular protein Obstructor-E (Obst-E) is needed for ridge formation at the interface between the procuticle and the apical plasma membrane of epidermal cells [16]. These ridges are missing in *obst-E* mutant larvae that by consequence do not contract during pupariation. The question is whether these ridges are altered in Tb^1 and $TwdlL^{93}$ mutant larvae. We analysed the basal site of the procuticle in wild-type, in Tb^1 and $TwdlL^{93}$ late third instar larvae by atomic force microscopy (AFM). The procuticle of wild-type larvae forms long convexities along the anteroposterior axis of the larva. The inner cuticular surface of in Tb^1 and $TwdlL^{93}$ larvae forms convexities that are comparably flat and disorganized (Fig. 10). Hence, Twdl proteins are needed for correct orientation of the procuticular basal ridges.

In these experiments, we also observed that the cuticular aggregates in Twdl mutant larvae influence the apical shape of the epidermal cells. We can therefore not decide whether the effect of Twdl on apical ridge formation is direct or indirect.

Localisation of the Obst-E does not depend on Twdl function

Both, Twdl and Obst-E proteins influence the formation of basal cuticular ridges. To test whether Twdl proteins may influence Obst-E localisation and function, we monitored Obst-E-GFP localisation in wild-type, in Tb^1 and $TwdlL^{93}$ late third instar larvae (Fig.10). In non-squat L3 larvae Obst-E-GFP is plainly localized in the procuticle. In Tb^1 and $Twdl^{93}$ larvae Obst-E-GFP localisation is unchanged, and does not bind to the Twdl aggregates (Fig.10). We conclude that the localisation of Obst-E does not depend on the function of Twdl proteins.

Discussion

ECMs and the ECM-producing cells adopt a concerted shape that is potentially important for tissue function. The insect integument consisting of the epidermis and the apical cuticle, for instance, conceivably plays a key role in body shape

determination. The two Twdl-class cuticle proteins Tb and TwdlD have been shown to be involved in this process in *D. melanogaster* [10].

Twdl proteins form 2-dimentional sheets within the epicuticle

Live imaging experiments with fluorescent-tagged proteins using CLSM reveal that Tb, TwdlF and TwdlS proteins form two 2D-dimesional adjacent horizontal sheets i.e. the TwdlF and the Tb/TwdlS sheets underneath the surface and above the procuticle. This localisation indicates that Twdl proteins possibly the epicuticle. In agreement with this interpretation, in ecdysone biosynthesis mutants where the epicuticle is absent [12], *twdl* gene expression is strongly reduced. We also conclude that the uniform appearance of the epicuticle in electron-micrographs does not reflect the stratified organisation revealed by fluorescence CLSM. Thus, the epicuticle is a more complex structure than supposed by mere ultrastructure analysis.
Dominant mutations in *twdl* genes provoke mis-localisation of the mutated proteins and their accumulation as 3-dimensional aggregates within the procuticle. Non-mutated Twdl proteins are incorporated into these structures. Based on these data we assume that Twdl proteins interact with each other. These observations argue that the mutated Twdl protein sequence loses its ability to form a flat 2-dimensional ECM but recruits normal and mutated protein sequences to form ectopic 3-dimensional aggregates without losing the ability to self-assemble. The recruitment, however, is selective, i.e. not all Twdl proteins tested are attracted to these aggregates. In addition, mutant Twdl proteins attract dityrosinylated proteins from the epicuticle-procuticle interface. This supports the notion that Twdl protein polymers are responsible for the formation and orientation of the adjacent dityrosine sub-layer including Resilin that is assumed to confer elasticity.
In summary, the epicuticle consists of polymers of Twdl proteins that partition this layer into 2-dimensional horizontal sheets by self-assembly.

Squat body shape as a consequence of body wall tension changes

Our data underline that Twdl proteins play a key role in body shape determination or maintenance. This function might rely on their localisation and function within the cuticle. Alternatively, the dominant phenotype caused by *Twdl* mutations, however, suggests that the defects may be neomorphic, i.e. they might be unrelated to the normal function of these proteins. Together, three possible scenarios can explain the mechanism of Twdl protein function in body shape implementation: 1) the “cytoplasmic”, 2) “epidermal-cuticular interface” and 3) the “cuticle” scenario.
The “cytoplasmic” theory relies on mutated Twdl proteins that fail to be transported to the cuticle but accumulate in cytoplasmic structures, probably vesicles, during cuticle formation when massive secretion and vesicle sorting occur [5, 20]. Accumulation of Twdl-vesicles may perturb plasma membrane dynamics, and thereby cause loss of correct cell shape along the antero-posterior axis. The altered cell shape would, in turn, influence the body shape.
The alternative “epidermal-cuticular” theory relies on the extracellular Twdl aggregates that are in close contact with the apical surface of the epidermal cells. According to this theory, these aggregates in the procuticle are responsible for the dis-organisation of the regular ridges that run along the anteroposterior axis in the epidermal-cuticular interface [16]. These ridges have recently been shown to depend on the presence of the procuticular protein Obst-E that controls longitudinal contraction and lateral expansion of the L3 larvae during pupariation. The deletion of *obst-E* causes flattening of the ridges and formation of longer and thinner pupae. In *twdl* mutant larvae, Obst-E localisation appears to be normal. We therefore reckon

that body shape changes in *twdl* mutant animals are independent of Obst-E function. As a consequence of ridge mis-orientation in *twdl* mutant larvae, however, the epidermal cells lose their longitudinal antero-posterior direction and adopt a shape with random orientation. Accordingly, the change of orientation preference of epidermal cells may be responsible for the overall shorter but thicker body shape.

The third, “cuticle” theory considers the depletion of either the epicuticle itself or the epicuticle-procuticle interface might be the reason for the aberrant body shape in *twdl* mutant animals. In this view, the Twdl polymers and/or the dityrosynilated proteins of the epicuticle-procuticle interface confer the elastic forces resisting the internal hydrostatic pressure. A thin epicuticle and/or epicuticle-procuticle sub-layer may be insufficient to withstand these forces. According to the formula of Barlow, a weakened wall of a closed pipe or cylinder would allow radial rather than longitudinal expansion of the object (Fig. 11). In analogy, due to a weakened cuticle and assuming a normal hydrostatic pressure, *twdl* mutant larvae become thick and short. Epidermal cells would, in this scenario, passively follow cuticle stretching in the lateral direction.

In any case, body shape change in *twdl* mutant larvae does not affect locomotion efficiency. Importantly, the *twdl* mutant phenotype enables us distinguishing body shape and locomotion as distinct functions of the cuticle that are not necessarily linked.

Twdl evolution

The *D. melanogaster* genome encodes 27 *twdl* genes. Different combination of the respective proteins in different body regions allow establishment of different types of epicuticles, thereby, conform with our “cuticle” theory, probably influencing the physical properties of the cuticle. So far so good. In contrast to *D. melanogaster* some insects such as the bedbug *Cimex lectularius* or the honeybee *Apis mellifera* do only have two or three copies of *twdl* in their genome [21]. How is epicuticle complexity that we encounter in *D. melanogaster* achieved in these species? We can only speculate that, testified by the varying number of *twdl* genes, the epicuticle is a fast evolving structure and therefore reckon that other types of epicuticular proteins may contribute to its construction to accommodate its different functions in species with only a few *twdl* genes.

References

1. Kiani C, Chen L, Wu YJ, Yee AJ, Yang BB. Structure and function of aggrecan. Cell Res. 2002;12(1):19-32. Epub 2002/04/11. doi: 10.1038/sj.cr.7290106. PubMed PMID: 11942407.
2. Horkay F. Interactions of Cartilage Extracellular Matrix Macromolecules. J Polym Sci B Polym Phys. 2012;50(24):1699-705. Epub 2013/09/03. doi: 10.1002/polb.23191. PubMed PMID: 23997426; PubMed Central PMCID: PMCPMC3755958.
3. Horkay F, Basser PJ, Hecht AM, Geissler E. Hierarchical organization of cartilage proteoglycans. Macromol Symp. 2011;306-307(1):11-7. Epub 2011/09/01. doi: 10.1002/masy.201000115. PubMed PMID: 23565043; PubMed Central PMCID: PMCPMC3615634.
4. Horkay F, Basser PJ, Hecht AM, Geissler E. Structure and Properties of Cartilage Proteoglycans. Macromol Symp. 2017;372(1):43-50. Epub 2018/05/08. doi: 10.1002/masy.201700014. PubMed PMID: 29731595; PubMed Central PMCID: PMCPMC5931741.

5. Moussian B. Recent advances in understanding mechanisms of insect cuticle differentiation. Insect Biochem Mol Biol. 2010;40(5):363-75. Epub 2010/03/30. doi: S0965-1748(10)00070-6 [pii]
10.1016/j.ibmb.2010.03.003. PubMed PMID: 20347980.
6. Moussian B. The Arthropod Cuticle. In: Minelli A, Boxshall G, Fusco G, editors. Arthropod Biology and Evolution. Berlin Heidelberg: Springer-Verlag; 2013. p. 171-96.
7. Noh MY, Kramer KJ, Muthukrishnan S, Kanost MR, Beeman RW, Arakane Y. Two major cuticular proteins are required for assembly of horizontal laminae and vertical pore canals in rigid cuticle of Tribolium castaneum. Insect Biochem Mol Biol. 2014;53:22-9. doi: 10.1016/j.ibmb.2014.07.005. PubMed PMID: 25042128.
8. Mun S, Noh MY, Dittmer NT, Muthukrishnan S, Kramer KJ, Kanost MR, et al. Cuticular protein with a low complexity sequence becomes cross-linked during insect cuticle sclerotization and is required for the adult molt. Scientific reports. 2015;5:10484. doi: 10.1038/srep10484. PubMed PMID: 25994234; PubMed Central PMCID: PMCPMC4440208.
9. Shaik KS, Meyer F, Vazquez AV, Flotenmeyer M, Cerdan ME, Moussian B. delta-Aminolevulinate synthase is required for apical transcellular barrier formation in the skin of the Drosophila larva. Eur J Cell Biol. 2012;91(3):204-15. Epub 2012/02/02. doi: S0171-9335(11)00223-8 [pii]
10.1016/j.ejcb.2011.11.005. PubMed PMID: 22293958.
10. Guan X, Middlebrooks BW, Alexander S, Wasserman SA. Mutation of TweedleD, a member of an unconventional cuticle protein family, alters body shape in Drosophila. Proc Natl Acad Sci U S A. 2006;103(45):16794-9. Epub 2006/11/01. doi: 0607616103 [pii]
10.1073/pnas.0607616103. PubMed PMID: 17075064; PubMed Central PMCID: PMC1636534.
11. Hartenstein V, Campos-Ortega JA. The embryonic development of *Drosophila melanogaster*. Berlin ; New York: Springer-Verlag; 1985. 227 p.
12. Gangishetti U, Veerkamp J, Bezdan D, Schwarz H, Lohmann I, Moussian B. The transcription factor Grainy head and the steroid hormone ecdysone cooperate during differentiation of the skin of Drosophila melanogaster. Insect Mol Biol. 2012;21(3):283-95. Epub 2012/03/31. doi: 10.1111/j.1365-2583.2012.01134.x. PubMed PMID: 22458773.
13. Ejsmont RK, Sarov M, Winkler S, Lipinski KA, Tomancak P. A toolkit for high-throughput, cross-species gene engineering in Drosophila. Nat Methods. 2009;6(6):435-7. Epub 2009/05/26. doi: nmeth.1334 [pii]
10.1038/nmeth.1334. PubMed PMID: 19465918.
14. Pina C, Pignoni F. Tubby-RFP balancers for developmental analysis: FM7c 2xTb-RFP, CyO 2xTb-RFP, and TM3 2xTb-RFP. Genesis. 2012;50(2):119-23. doi: 10.1002/dvg.20801. PubMed PMID: 21913310; PubMed Central PMCID: PMCPMC3931234.
15. Forster D, Armbruster K, Luschnig S. Sec24-dependent secretion drives cell-autonomous expansion of tracheal tubes in Drosophila. Curr Biol. 2010;20(1):62-8. Epub 2010/01/05. doi: S0960-9822(09)02079-X [pii]
10.1016/j.cub.2009.11.062. PubMed PMID: 20045324.
16. Tajiri R, Ogawa N, Fujiwara H, Kojima T. Mechanical Control of Whole Body Shape by a Single Cuticular Protein Obstructor-E in Drosophila melanogaster. PLoS Genet. 2017;13(1):e1006548. doi: 10.1371/journal.pgen.1006548. PubMed PMID: 28076349; PubMed Central PMCID: PMCPMC5226733.

17. Moussian B, Schwarz H. Preservation of plasma membrane ultrastructure in Drosophila embryos and larvae prepared by high-pressure freezing and freeze-substitution. Drosophila Information Service. 2010;93:215-9.
18. Zuber R, Shaik KS, Meyer F, Ho HN, Speidel A, Gehring N, et al. The putative C-type lectin Schlaff ensures epidermal barrier compactness in Drosophila. Scientific reports. 2019;9(1):5374. doi: 10.1038/s41598-019-41734-9. PubMed PMID: 30926832; PubMed Central PMCID: PMCPMC6440989.
19. Fristrom D, Doctor J, Fristrom JW. Procuticle proteins and chitin-like material in the inner epicuticle of the Drosophila pupal cuticle. Tissue Cell. 1986;18(4):531-43. Epub 1986/01/01. doi: 0040-8166(86)90019-4 [pii]. PubMed PMID: 3092400.
20. Moussian B, Veerkamp J, Muller U, Schwarz H. Assembly of the Drosophila larval exoskeleton requires controlled secretion and shaping of the apical plasma membrane. Matrix Biol. 2007;26(5):337-47. Epub 2007/03/16. doi: S0945-053X(07)00020-0 [pii]
10.1016/j.matbio.2007.02.001. PubMed PMID: 17360167.
21. Soares MP, Silva-Torres FA, Elias-Neto M, Nunes FM, Simoes ZL, Bitondi MM. Ecdysteroid-dependent expression of the tweedle and peroxidase genes during adult cuticle formation in the honey bee, Apis mellifera. PLoS One. 2011;6(5):e20513. Epub 2011/06/10. doi: 10.1371/journal.pone.0020513
PONE-D-11-03904 [pii]. PubMed PMID: 21655217; PubMed Central PMCID: PMC3105072.

Figure legends

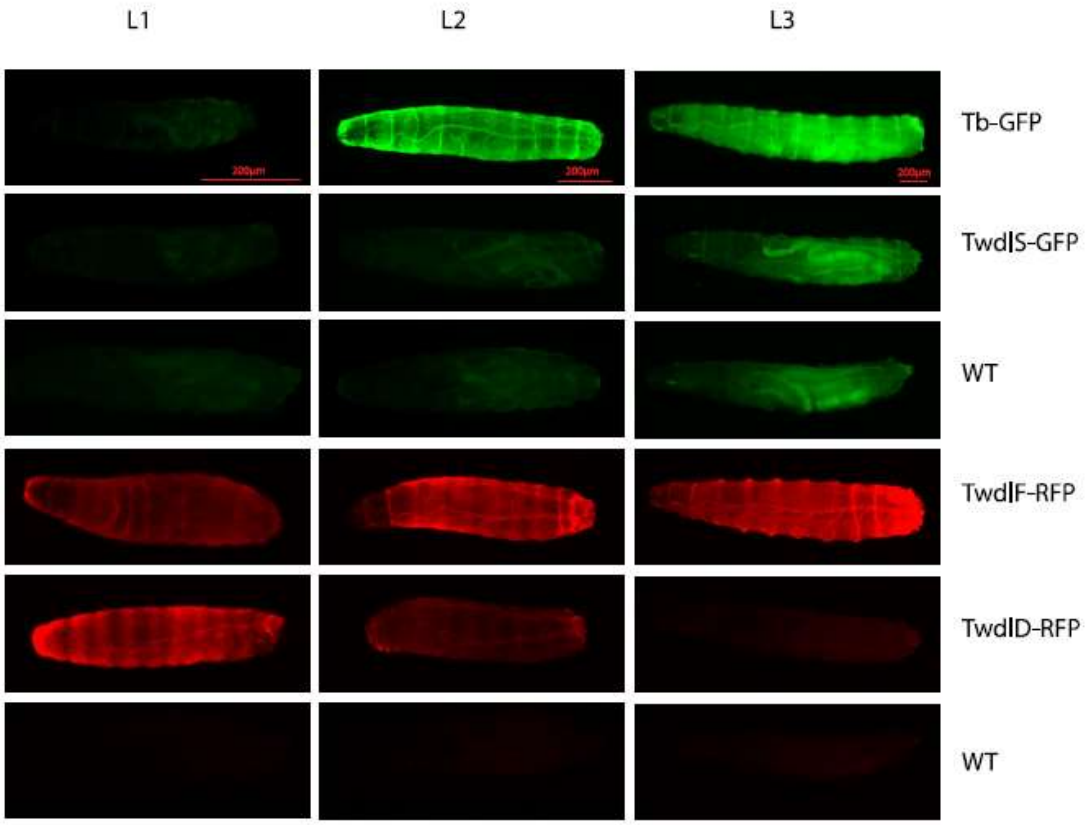

Fig. 1. Expression profile of GFP- and dsRed-tagged Twdl proteins at three larval stages.

All four Twdl proteins localize to the larval cuticle. Tb-GFP is weakly visible at first larval stage (L1) as lateral patches, whilst at second (L2) and third (L3) larval stages is decently visible in the whole cuticle. The signal of TwdlS-GFP is very faint in the cuticle of L2 and weak in the whole cuticle of L3. TwdlF-RFP is observable in the entire cuticle at all larval stages. TwdlD-RFP shows strong striped signal in the cuticle of L1, weaker in L2 and very faint signal in the posterior cuticle of L3 larvae.

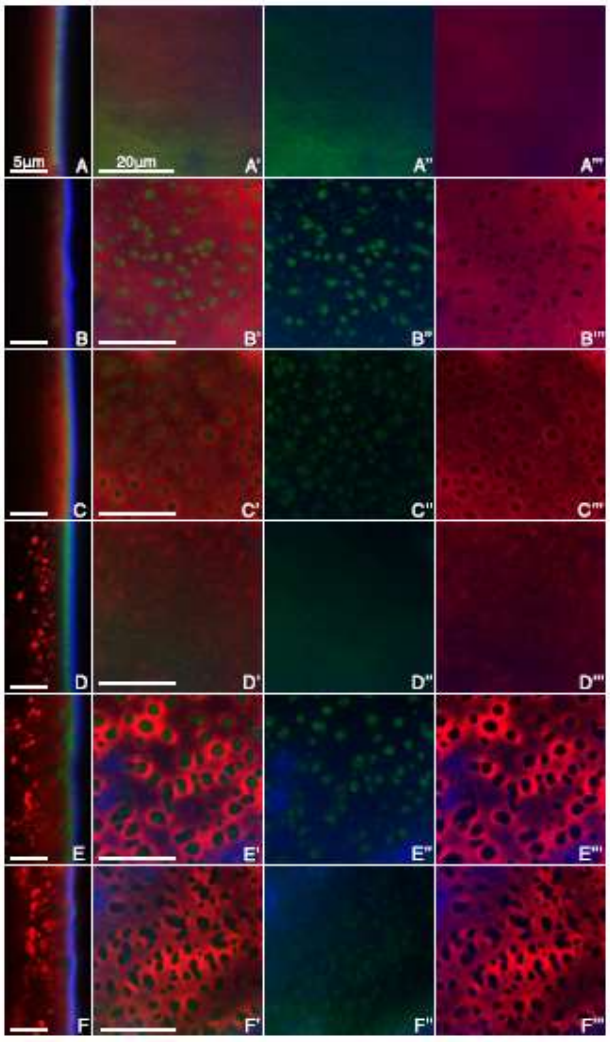

Fig. 2. Localisation of TwdlS-GFP, Cpr67b-RFP and Verm-RFP in the cuticle of non-Tb, Tb1 and Tb93 third instar larvae.

In the cuticle of non-Tb larvae, TwdlS-GFP (green) is uniformly distributed forming thin layer under the blue 405-induced autofluorescent line (A and D: lateral views; A'-A''' and D'-D'''top views with respective channels separation). dsRed-tagged chitin-binding Cuticular Protein 67b (Cpr67b-dsRed, red), expressed in the epidermis from the TwdlM promoter is plainly distributed in the thick procuticle under the TwdlS-GFP layer (A-A'''). Ubiquitously expressed Vermiform-RFP (Verm-RFP, red) is plainly distributed in the entire procuticle below the TwdlS-GFP layer and forms vesicle-like structures in the cells (D-D'''). In the cuticle of Tb1 larvae (B-B'''; E-E''') and Tb93 larvae (C-C'''; F-F''') TwdlS-GFP partially localizes to the upper epicuticle, and partially binds to the aggregates immersed in the procuticle. It does not overlap with CPR67-dsRed (B-B'''; C-C''') and Verm-RFP (E-E'''; F-F'''), there are distinct borders between these proteins in the procuticle.

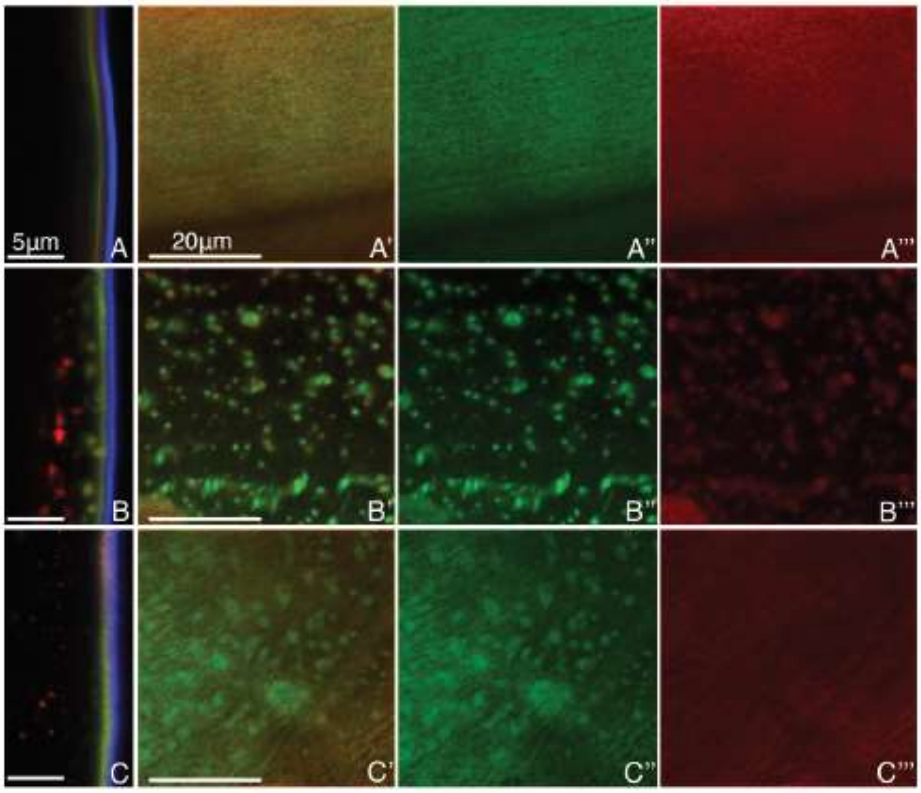

Fig. 3. Localisation of TwdlS-GFP and TwdlF-dsRed in the cuticle of non-Tb, Tb1 and Tb93 third instar larvae.

TwdlF-dsRed (red) and TwdlS-GFP (green) form two separate layers in the cuticle of WT larvae: TwdlF localizes just below the 405 layer and TwdlS-GFP under the TwdlF layer (A: lateral view, A'-A''': top views with respective channels separation). In the Tb1 larvae both proteins are partially mislocalised, forming aggregates in the lower cuticular layer (B-B'''). In the Tb93 larvae only part of TwdlS-GFP binds to the aggregates, but TwdlF-RFP does not (C-C'''). However, there is no decent stratification of these two proteins in the lateral view of the naked cuticle visible (C).

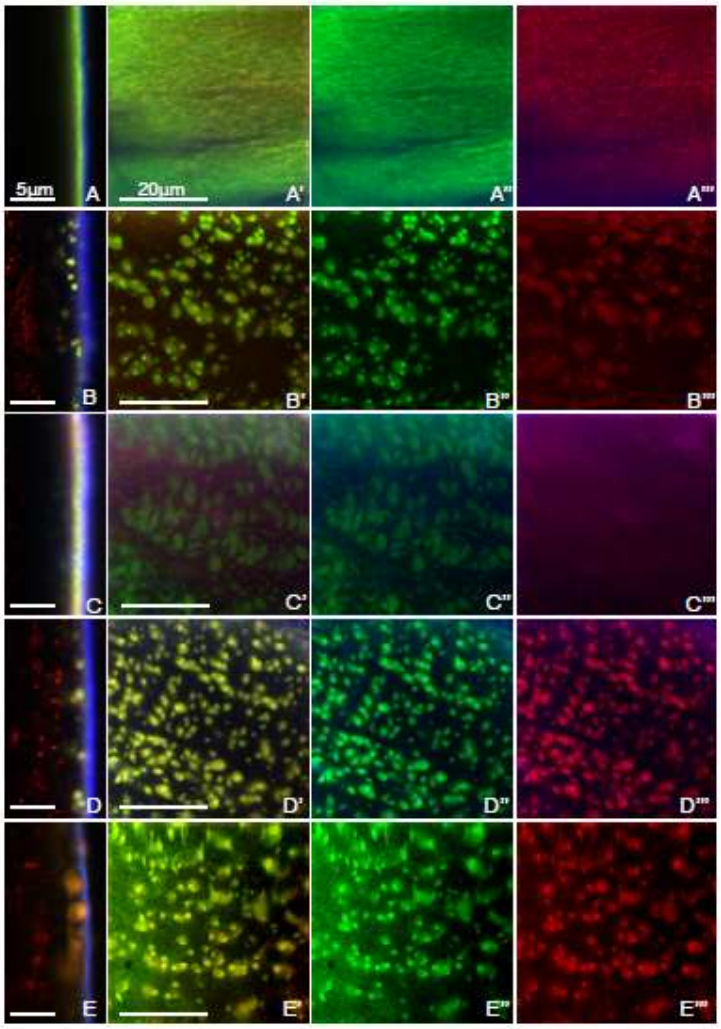

Fig.4. Localisation of Tb-GFP, TwdlF-dsRed and TwdlS-GFP in the cuticle of non-Tb and Tb mutant larvae.

In the cuticle of WT larvae Tb-GFP (green) and TwdlF-dsRed (red) overlap (A: lateral view, A'-A''': the top views with respective channels separation). In the cuticle of Tb1 larvae both proteins are partially aggregated (B-B'''). In the cuticle of Tb93 larvae Tb-GFP forms aggregates, whilst TwdlF-dsRed does not or very weakly (C-C'''). In the cuticle of the larvae with two additional copies of RFP-tagged, mutated Tb protein (Tb1-RFP, red), the non-mutated Tb-GFP form (green) binds to the aggregates formed by Tb1-RFP (D-D'''). TwdlS-GFP protein (green) joins the Tb1-RFP aggregates as well (E-E''').

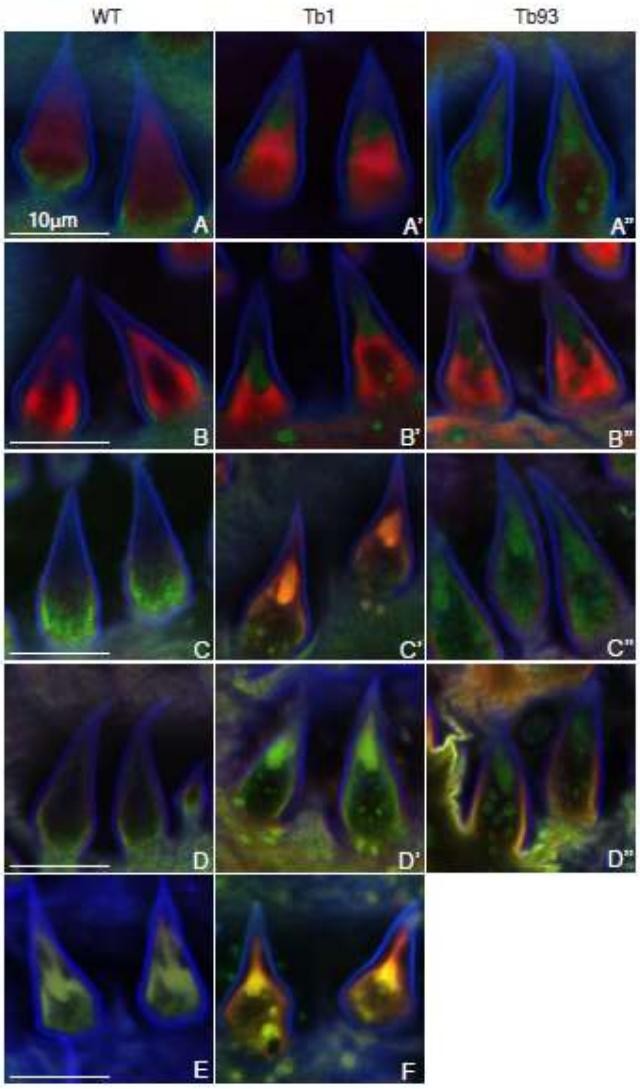

Fig. 5. Localisation of Twdl fluorescent proteins in the hairs of non-Tb and Tb mutant larvae.

In the dorsal hairs of non-Tb larvae TwdlS-GFP forms a layer under the autofluorescent line (blue) at the bases of the hairs but does not reach their tip (A, B). Cpr67b-dsRed (A) and Verm-RFP (B) are localised in the center of hairs. In the hairs of Tb1 and Tb93 larvae, TwdlS-GFP accumulates at the tips and forms smaller aggregates in the middle of the hair, whilst Cpr67b-dsRed and Verm-RFP are localised in the center, excluding the TwdlS areas (A'-A''; B'-B''). TwdlF-dsRed (red) forms a layer between the autofluorescent layer and TwdlS-GFP layer (green) in the hairs of non-Tb larvae (C). In the hairs of Tb1 larvae stratification under the envelope seems to be retained, whilst at the hair tip and in the aggregates proteins overlap (C'). In Tb93 larvae stratification is retained and only TwdlS-GFP is mislocalized (C''). Localisation of Tb-GFP (green) in the hairs of non-Tb and Tb larvae is similar to TwdlS-GFP (D-D''). Mutated Tb1-RFP (red) form attracts unmutated Tb-GFP (E,

green) and TwdlS-GFP (F, green).

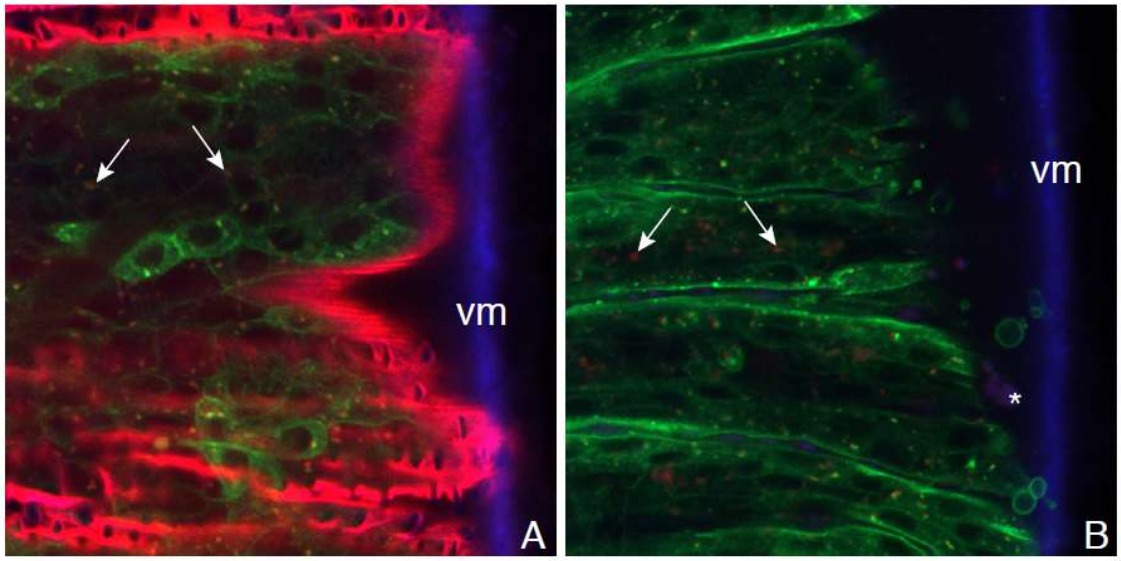

Fig.6 Localisation of TwdlF-dsRed in WT and phm mutant larvae.

In the wild type first instar larvae before hatching the signal of TwdlF-dsRed (red) is strong in the entire cuticle and in the round-shaped cellular structures (shown by arrows), probably vesicles (A; green: ubiquitously produced membrane-binding CD8-GFP; blue: 405-induced cuticle and vitelline membrane (vm) autofluorescence). In the phantom mutants expression of TwdlF-dsRed is very low, there is weak red signal corresponding to the cellular vesicles and unusual structures outside the epidermis, not attached to the body surface (shown by asteriks), containing also the 405-induced material (B). In this case, the 405-induced autofluorescent signal is also strongly diminished in the whole cuticle.

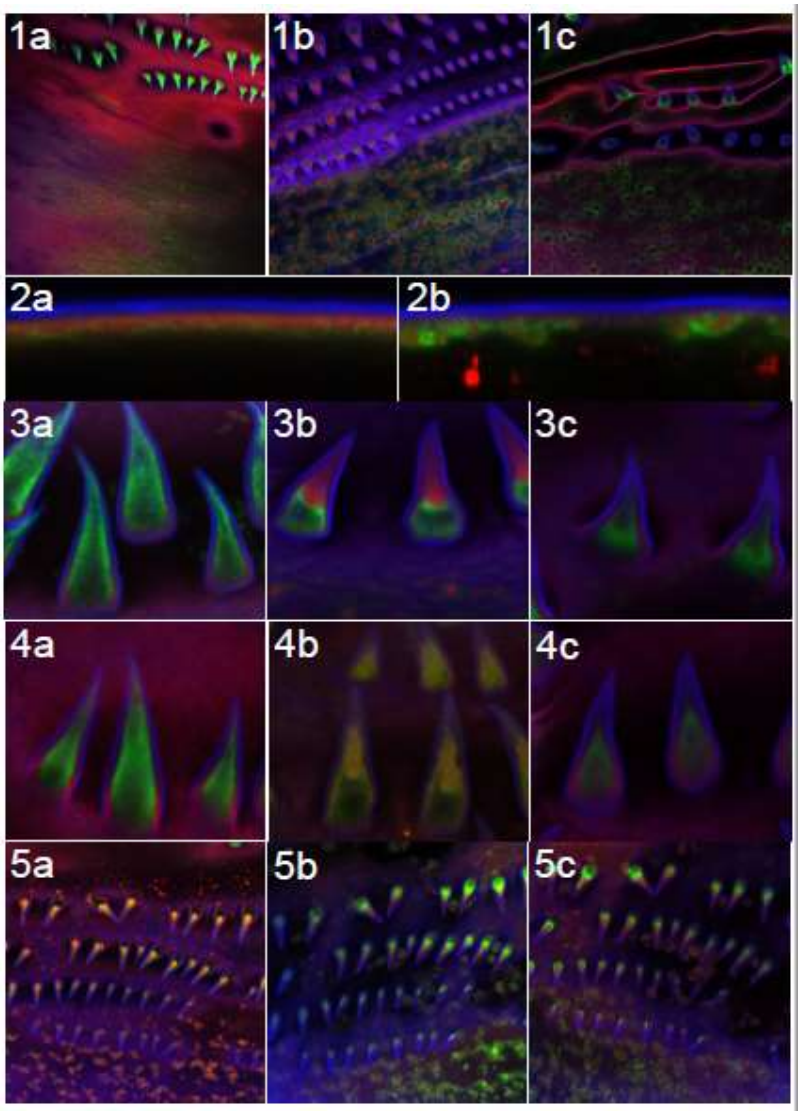

Fig. 7. Localisation of Resilin-Venus in wild type, Tb1, Tb93 larvae.

In the *wild-type* third instar larvae Resilin-Venus localizes beneath the TwdlF-dsRed layer (1a, 2a). In the Tb^{1} (1b, 2b) and Tb^{93} (1c) mutant larvae Resilin-Venus is attracted to the aggregates and encircles them. In the dorsal hairs of the young *wild type* third instar larvae just after hatching Resilin-Venus occupies the space below the TwdlF-dsRed layer (4a), whilst in the hairs of the Tb^{1} and Tb^{93} mutant larvae (4b and 4c, respectively), it accumulates also at the hair tips, overlapping with the aggregates. In one-day-old third instar *wild-type* larvae Resilin-Venus localisation is unchanged compared to young third instar larvae (3a), whilst in one-day-old Tb^{1} and Tb^{93} mutant larvae (3b and 3c, respectively) Resilin-Venus is not localised at the hair tips but encases the Twdl-aggregates at the hair tip. Changes of Resilin-Venus localization occurring with time can be visualized in one region of a living L3 Tb1 larva just after hatching (5a), 24 hours after hatching (5b) and 48 hours after hatching (5c).

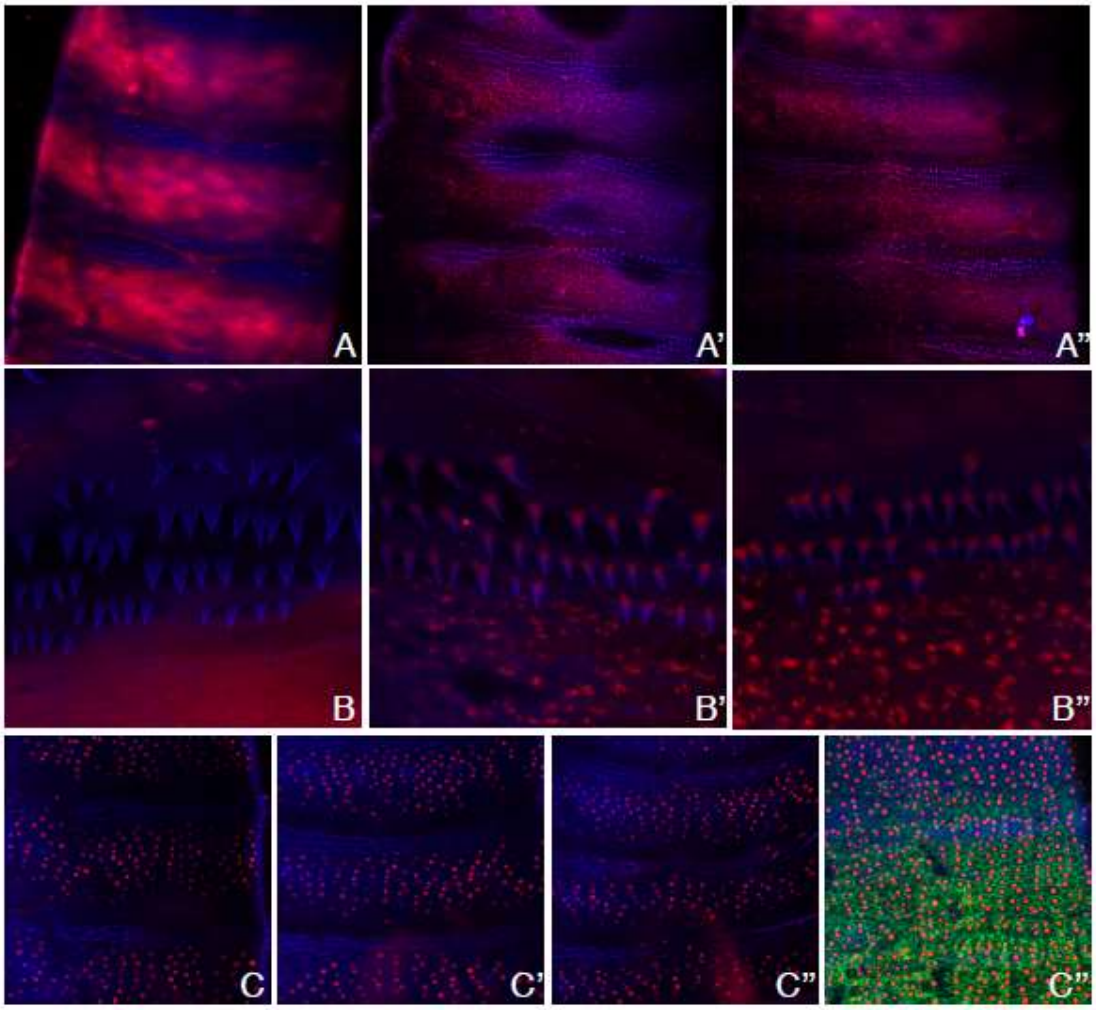

Fig.8 Non-cell autonomous localization of the aggregated Twdls in the cuticle.

On the dorsal side of the non-Tb L2 larvae TwdlD-dsRed is visible in striped domains of the naked cuticle, excluding the domains with hairs (A; B: magnification of the hair region). In the cuticle of Tb1(A', B') and Tb93 (A'', B'') mutant larvae the aggregates of the TwdlD-dsRed are observable in the whole cuticle, also in hairs. Red Fluorescent Protein with attached nuclear localisation signal, expressed from the TwdlD promoter (TwdlD>RFP-NLS) in the background of the non-Tb(C), Tb1 (C') and Tb93 (C'') larvae, in all three cases shows a striped pattern of red nuclei. In control larvae expressing Red Fluorescent Protein with an NLS signal in the whole cuticle, all epidermal red nuclei are visible (C'''; green: ubiquitously expressed membrane-binding CD8-GFP marks the cell boarders).

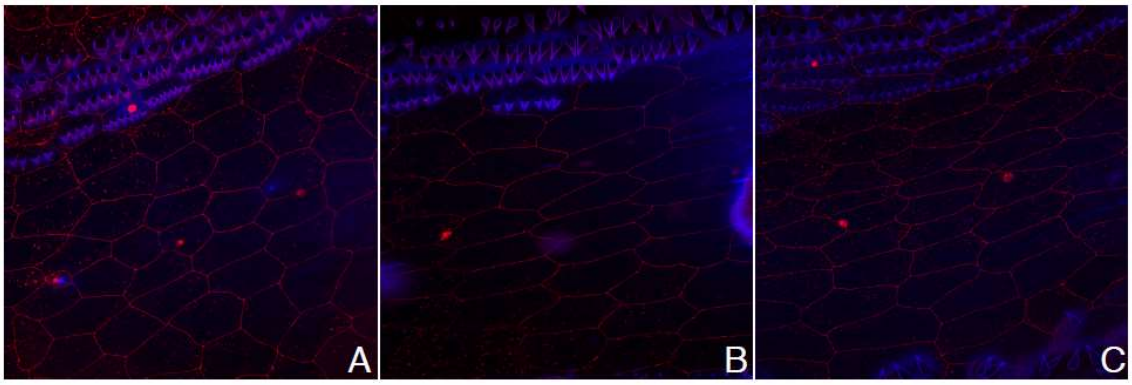

Fig. 9 The differences in the cell shape and cuticular internal surface of the non-Tb and Tb mutant larvae.

The expression of the fluorescent-tagged E-Cadherin (E-Cadherin-mCherry, red), accumulating at the borders of epidermal cells shows that the cells of the third instar Tb1 (A) and Tb93 (B) larvae are more flat longitudinally and more broad laterally compared to the wild-type epidermal cells (A). The signal strength of E-Cadherin is comparable at all cell borders, anterior, posterior and the lateral ones in the non-Tb and Tb mutant larvae.

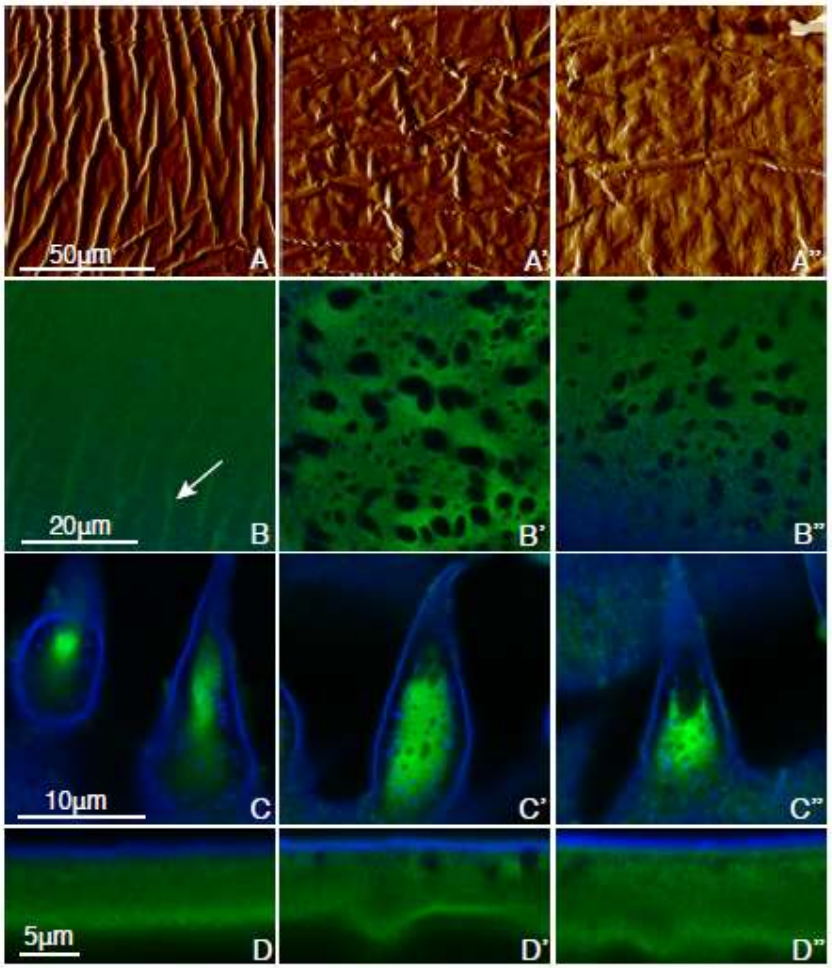

Fig.10 The structure of procuticular ridges but not the localisation of Obstructor-GFP is changed in Tb mutant larvae.

The internal cuticular surface of the non-Tb L3 larvae scanned by the atomic force microscope shows longitudinal ridges running parallel to the anterior-posterior axis (A). In the Tb1 (A') and Tb93 mutants (A'') the structure of the ridges is disrupted, they run in different directions and seem to be flatter.

GFP-tagged chitin binding protein Obstructor E (ObstE-GFP, green) is plainly distributed in the whole procuticle of the naked cuticle (B: the top view of the dorsal cuticle; D: the lateral view; blue: autofluorescence of the external cuticular envelope) and in the center of the dorsal hairs of wild type larvae (C). On the top view the cuticular ridges are discernable (B, marked with arrow). In the Tb1 (B'-D') and the Tb93 larvae (B''-D'') it is still plainly distributed in the procuticle, excluding the epicuticular aggregates.

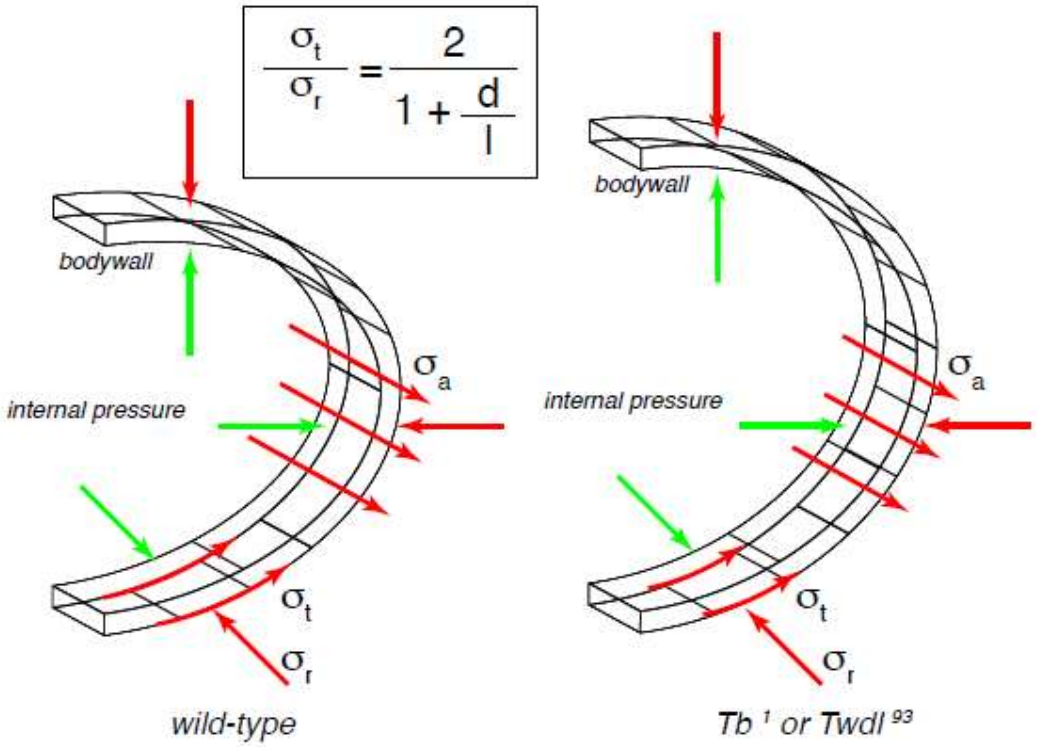

Fig. 11 Explanation of a growth of mutated Tweedle larvae according to Barlow's law.

According to the law of Barlow, an object of the shape of a closed pipe or cylinder with a weakened wall will expand rather radially than longitudinally. In analogy, the Tweedle mutants with depleted epicuticle will become thicker and shorter during growth than the wild type larvae. d= diameter of the object, σa = axial tension (longitudinal direction) in the wall, σt = tangential tension in the wall, σr= radial tension, l = length of the object.

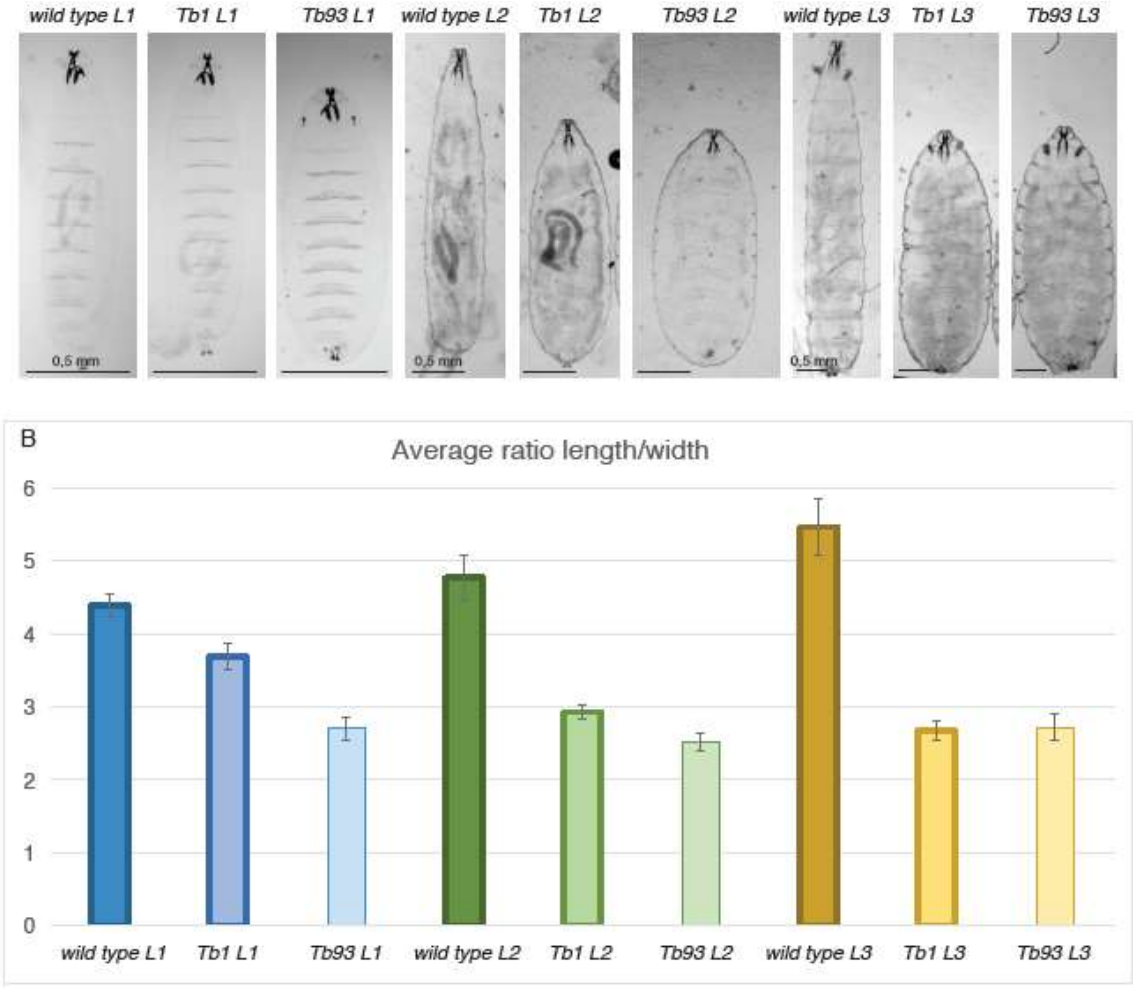

Suppl. Fig.1 Comparison of the shape of the wild type, Tb1 and Tb93 theree larval stages.

Hoyer's preps of the larval cuticles reveal that the the first, second and third instar Tb93 larvae are decently shorter and thicker than the wild type larvae (A). Second and third instar Tb1 larvae are clearly shorter and thiker, but the first instar larvae are only a little bit shorter than the wild type larvae (A). The shape differences between Tb and wild type larvae become more visible at every subsequent stage. B: The average ratio of length to the width of measured cuticle preps of the wild type, Tb1 and Tb93 first, second and third instar larvae.

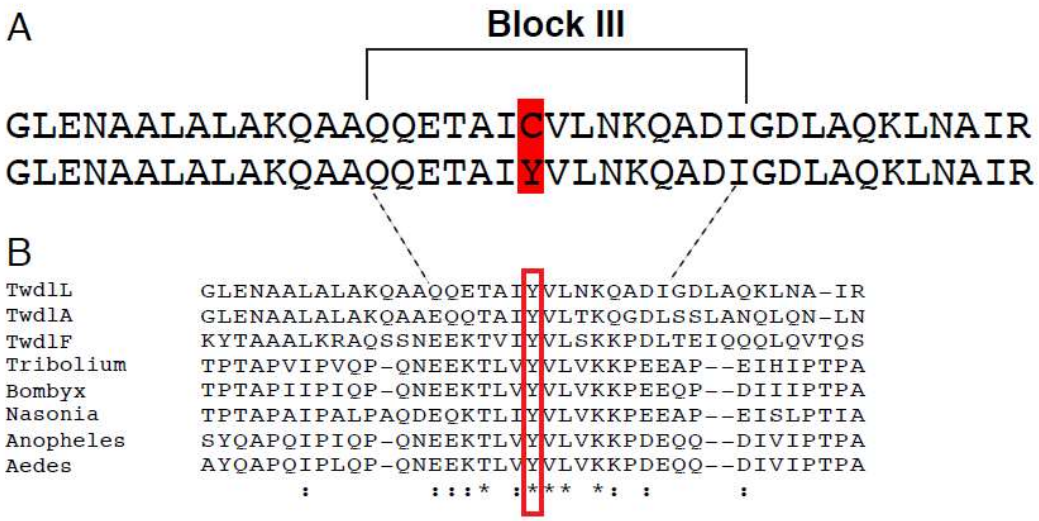

Suppl. Fig. 2. Tb93 allele is a TwdlL allele.

In a conserved block III of a DUF 243 domain of the TwdlL protein in Tb93 larvae there is a missense mutation changing tyrosine into cysteine (A, mark on red). This tyrosine is conserved in the Twdl proteins of many insect species (B, conserved tyrosine marked with red frame).

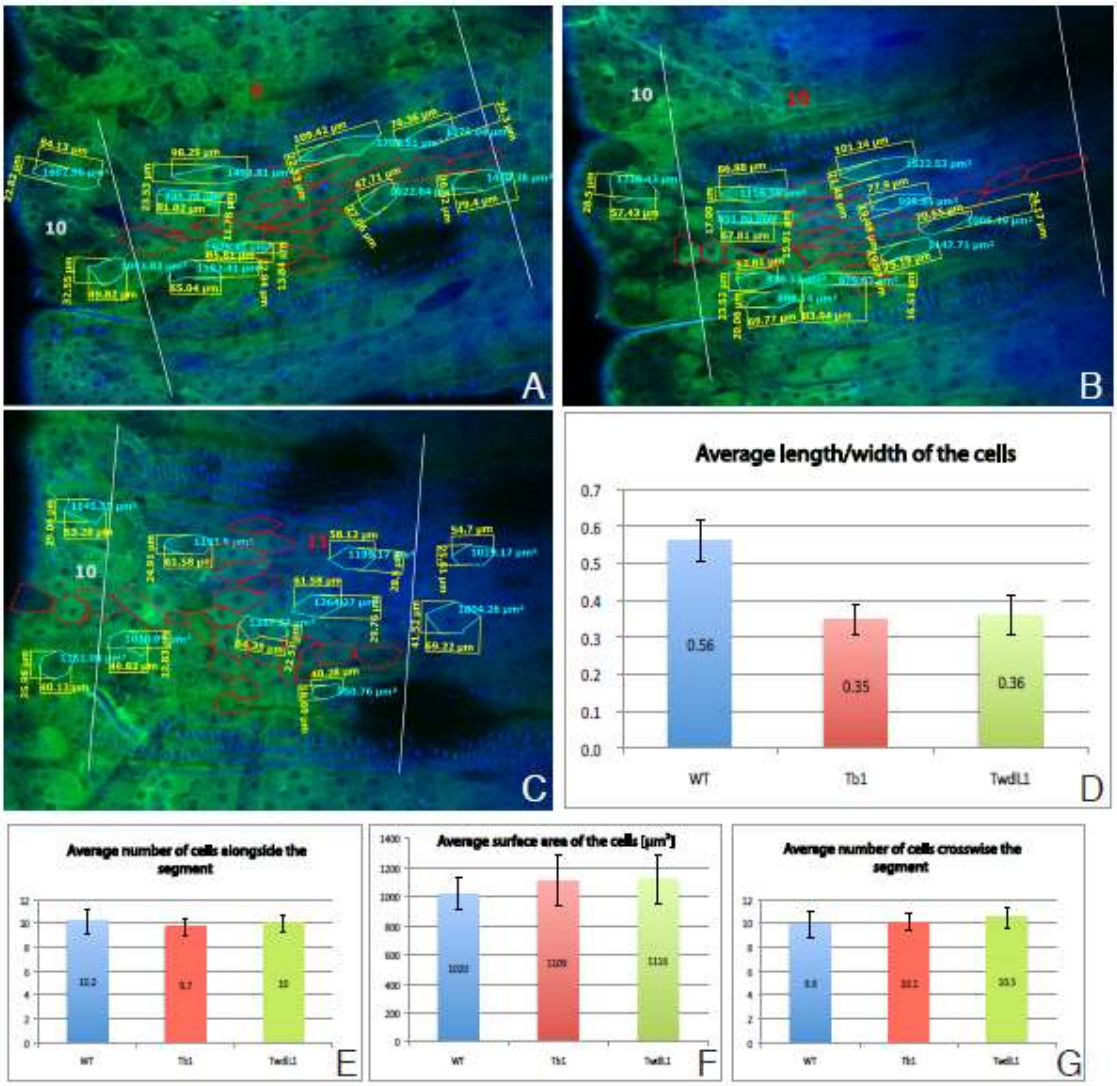

Suppl. Fig. 3. Comparison of the cell shape and the cell number in wild type, Tb1 and Tb93 third instar larvae.

In the larval third abdominal segment the average cell number along the whole segment (between the two apical areas with hairs) and across half of the segment is comparable in the apical epidermis of the wild type, Tb1 and Tb93 mutant larvae (A, B and C, respectively; Borders of counted cells marked on red. Green: ubiquitously expressed membranous CD8-GFP, blue: 405-induced cuticle autofluorescence; E, G). The average cell area also does not differ between all three cases (A-C: borders of the cells with measured area and the outcome marked on blue; F). The ratio of the length to the width of the epidermal cells of the Tb larvae is significantly lower compared to the ratio of the non-Tb epidermal cells (A-C: measurements of the length and the width marked on yellow; D).

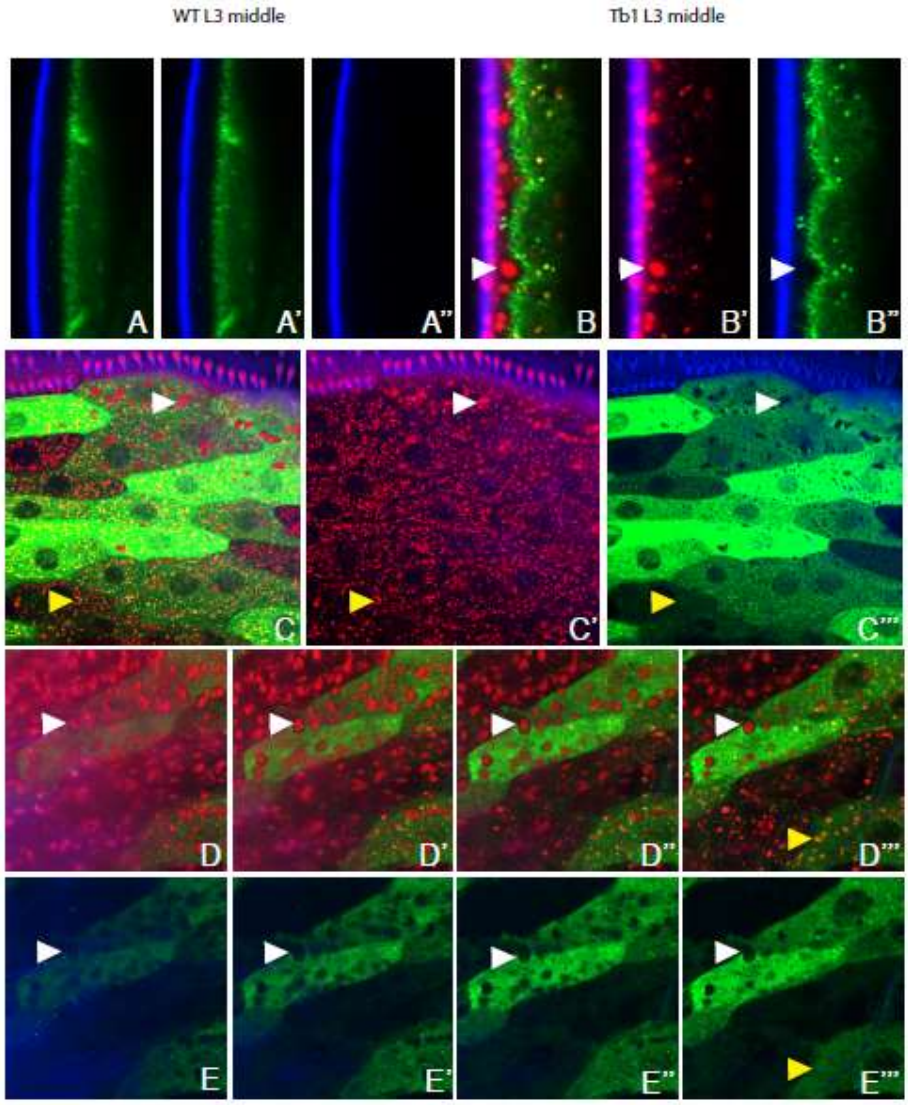

Suppl. Fig.4 Influence of the ectopic Twdl aggregates on the epidermal apical surface

The apical epidermal surface in wild type third instar larvae is even (A-A'', green: ubiquitously expressed membranous CD8-GFP marking the apical cell surface, blue: autofluorescent 405-induced envelope; A': without red channel; A'': without green channel). Tb1-RFP aggregates (red) accumulating ectopically in the procuticle cause the convexities in the epidermal cell surface (B-B''; without red (B') and green channel (B'')); convexity shown by a white arrow). C-C'': the top view, convexities in the epidermal apical surface shown by a white arrow, whilst the cellular Tb1-RFP aggregates shown by a yellow arrow. D-D''': Z-stack of the epidermal cells from the top view with higher magnification, showing procuticular aggregates and the cellular aggregates inside the cell. E-E''': Z-stack without a red channel, revealing holes in the epidermal surface in the places of the procuticular aggregates.

	WT1	WT2	WT3	WT4	WT5	Tb1 1	Tb1 2	Tb1 3	Tb1 4	Tb1 5	Tb93 1	Tb93 2	Tb93 3	Tb93 4	Tb93 5
longest	190.43	188.4	187.97	186.75	180.35	117.69	117.89	101.32	98.08	96.57	108.47	103.77	106.45	116.25	107
shortest	163.23	163.32	167.29	162.53	160.59	98.08	102.83	91.21	87.01	90.25	98.62	89.94	95.41	107.79	91.92
% shortest/longest	85.72	86.69	89.00	87.03	89.04	83.34	87.23	90.02	88.71	93.46	90.92	86.67	89.63	92.72	85.91
			87.50					88.55					89.17		
SD	1.47373					3.714186					2.862643				

	WT					Tb1					Tb93				
	1	2	3	4	5	1	2	3	4	5	1	2	3	4	5
1	3	10	43	22	4	13	7	26	16	15	20	0	0	0	0
2	18	28	5	18	23	23	13	27	20	14	8	0	0	0	0
3	17	13	11	11	33	32	15	5	35	33	17	15	0	0	0
4	18	23	32	13	3	25	4	8	41	37	35	33	1	49	34
5	24	24	32	27	22	31	17	13	25	30	45	43	23	32	34
6	26	3	20	3	10	20	33	16	30	5	18	43	28	12	26
7	27	15	21	15	19	10	28	6	12	7	41	47	40	25	23
8	42	30	26	10	27	7	28	10	30	30	41	13	41	1	23
9	28	6	2	43	5	12	20	20	46	38	3	13	10	25	48
10	43	10	8	47	18	26	1	28	2	44	3	13	18	16	15
11	3	32	13	25	20	10	5	30	25	10	24	4	24	1	40
12	8	6	26	5	42	6	8	35	28	17	23	21	10	7	36
13	34	5	28	14	27	12	15	35	3	22	13	45	27	7	19
14	36	22	10	3	27	18	17	20	8	13	35	5	21	35	21
15	27	5	14	7	18	35	26	6	13	28	16	20	8	46	28
16	32	5	23	9	22	18	40	25	50	37	16	22	22	1	48
17	45	7	35	46	34	17	38	45	27	17	19	42	48	10	54
18	42	53	59	41	54	2	31	12	22	13	33	28	32	33	32
19	33	12	6	14	17	26	55	28	12	25	33	53	19	52	40
20			23	4	33	34	58	36	51			45	18	42	41
average	26.63	16.26	21.85	18.85	22.90	18.85	22.95	21.55	24.80	22.89	23.32	25.25	19.50	19.70	28.10
average from			21.30					22.21					23.17		
SD			3.96					2.21					3.68		

Suppl. Fig. 5 *Cuticle stretchability and movement capabilities of the wild type, Tb^{1} and $TwdlL^{93}$ larvae.*